

# Online Power and Time Allocation in MIMO Uplink Transmissions Powered by RF Wireless Energy Transfer

Kai Liang, Liqiang Zhao, *Member, IEEE*, Kun Yang, *Senior Member, IEEE*, and Xiaoli Chu, *Senior Member, IEEE*

**Abstract**—Wireless energy transfer (WET) has been a promising technology to tackle the lifetime bottlenecks of energy-limited wireless devices in recent years. In this paper, we study a WET-enabled multiple-input multiple-output system including a base station (BS) and a user equipment (UE), which has a finite battery capacity. We consider slotted transmissions, where each slot includes two phases, namely, a downlink (DL) WET phase and an uplink (UL) wireless information transmission (WIT) phase. In the WET phase (a fraction  $\tau$  of a slot), the BS transfers energy and the UE stores the received energy in the battery. In the WIT phase (a fraction  $1 - \tau$  of a slot), the UE transmits information to the BS by using the energy in the battery. Considering the power sensitivity  $\alpha$  of the radio frequency to DC conversion circuits, the BS transfers energy only if the UE received power is larger than  $\alpha$ , and the DL WET is formulated as a Bernoulli process. Based on the formulation, we propose an online power and time allocation algorithm to maximize the average data rate of UL WIT. We also extend the proposed algorithm to multiple user systems. The numerical results show that the proposed algorithm outperforms the existing schemes in terms of average data rate, energy efficiency, and outage probability.

**Index Terms**—Finite battery size, multiple-input multiple-output (MIMO), online power and time allocation, wireless energy transfer (WET).

## I. INTRODUCTION

ENERGY harvesting (EH) techniques can prolong the lifetime and improve the scalability of some energy constrained networks by capturing energy from the surrounding

Manuscript received February 7, 2016; revised June 18, 2016, July 25, 2016, and October 26, 2016; accepted December 27, 2016. Date of publication January 11, 2017; date of current version August 11, 2017. This work was supported in part by the National Natural Science Foundation of China under Grant 61372070, in part by the Natural Science Basic Research Plan in Shaanxi Province of China under Grant 2015JM6324, in part by the Ningbo Natural Science Foundation under Grant 2015A610117, in part by the Hong Kong, Macao and Taiwan Science and Technology Cooperation Program of China under Grant 2015DFT10160, and in part by the 111 Project (B08038). The review of this paper was coordinated by Dr. X. Dong.

K. Liang and L. Zhao are with the State Key Laboratory of Integrated Service Networks, Xidian University, Xi'an 710071, China (e-mail: klxdu@hotmail.com; lqzhao@mail.xidian.edu.cn).

K. Yang is with the School of Computer Science and Electronic Engineering, University of Essex, Colchester CO4 3SQ, U.K. (e-mail: kunyang@essex.ac.uk).

X. Chu is with the Department of Electronic and Electrical Engineering, The University of Sheffield, Sheffield S1 3JD, U.K. (e-mail: x.chu@sheffield.ac.uk).

Color versions of one or more of the figures in this paper are available online at <http://ieeexplore.ieee.org>.

Digital Object Identifier 10.1109/TVT.2017.2651949

environment, such as wind, solar, and radio frequency (RF) signals [1]. However, wind and solar energy availability is largely limited by the environment and weather, and thereby cannot provide wireless communication device with sustainable power supply.

On these ground, wireless energy transfer (WET), which is first carried out from Tesla's experiment a century ago [2], [3], has utilized to provide sustainable and controllable power supply for wireless devices recently. In accordance with the transmission distance, WET can be classified into two groups, namely, near-field and far-field WET, respectively. Near-field WET transmits energy through inductive coupling or magnetic resonance coupling featured with high-power density and conversion efficiency [4]. Nevertheless, the near-field WET is not appropriate for mobile and remote devices. The reasons are twofolds: first, the power strength of the near-field WET will be dramatically degraded with the increasing transmission distance [5]; and second, the near-field WET needs aligned induction coils or resonators at transmitters and receivers. In contrast, by capturing the RF radiation and converting it into a direct current (DC), RF WET, which is regarded as a far-field energy transfer technique, can provide service to mobile and remote devices. Hardware prototyping of RF-powered devices has been mainly developed for low-power-consumption applications [4], such as wireless sensor networks [6], health care and medical applications [7], and RF identification tags [8]. More complicated hardware design, which integrates information transmission technologies with RF WET, is urgently needed to testify the performance of RF-powered communications. For the aforementioned reasons, RF WET has attracted a lot of interest from both academia and industry [3], [4] and we emphasize our efforts on RF WET in this paper.

The offline power allocation for transmitters with finite capacity batteries powered by renewable energy sources was studied in [9] and [10]. These works indicated that the optimal offline solution aims to hold the longest stretches of constant power periods. Online energy management policies were studied for peer-to-peer data transmissions with EH transmitters [10], for hybrid energy supplies in point-to-point communications [11], and for multiple-input multiple-output (MIMO) systems [12]. A suboptimal resource allocation algorithm for maximizing energy efficiency in the orthogonal frequency division multiple access downlink (DL) of hybrid EH base stations (BSs) was

proposed in [13], assuming the knowledge of average time between two adjacent events (such as channel changes and energy arrivals).

A constant fractional power (FP) allocation policy for renewable energy powered single antenna transmissions was discussed in [14], which assumes a Bernoulli energy arriving process [15] with parameter  $p$  and fixed energy packet size  $E$ , without showing the rationality of this assumption or providing the accurate value of  $p$ .

Uplink (UL) wireless information transmission (WIT) powered by WET was studied in [16]–[20]. In [16], the massive MIMO system powered by WET adopted slotted transmissions, where each slot was divided into three phases for channel estimation, DL power transmission, and UL data transmission, respectively. In [17], a joint design of time allocation, energy beamforming, and UL power allocation was proposed to achieve rate fairness among users, where alternating optimization and nonnegative matrix theory were adopted to solve the nonconvex problem. The hybrid access point (H-AP) operating in full duplex mode was studied in [18], where H-AP transmits energy in the DL and receives information in the UL simultaneously. In [19], energy transferring nodes called power beacons (PBs) were used to power UL transmissions, and the relationship between the densities of BSs and PBs and the optimal UL transmission power for a given outage probability were obtained under a stochastic geometry model. Flint *et al.* [20] study three performance metrics: the expected EH rate, power outage probability, and transmission outage probability for performance analysis of ambient RF EH.

However, none of the above-mentioned works has taken into account the power sensitivity of RF-DC circuits. The received RF signals cannot be converted into DC (i.e., energy transfer) if their power level is lower than the power sensitivity of an RF-DC circuit [21]. Thus, actually received energy would be much lower than the theoretically predicted amount, leading to a falsely higher data rate. Besides, none of these works has considered the battery capacity, thus ignoring the possibility of energy overflow or the opportunities for the user equipment (UE) to optimize the use of harvested energy across UL WIT slots. In [16]–[18], the UE allocated all the harvested energy for the UL WIT in the current slot, and maximized single slot performance (such as data rates). This approach has been shown a lower data rate than the uniformly distributing energy between energy arrivals [9], [10].

To the best of our knowledge, few works have studied a WET-enabled communication system while considering both the power sensitivity of RF-DC circuits and the finite capacity battery. In this paper, we devise a power and time allocation algorithm for the MIMO UL transmission powered by WET, with the consideration of finite capacity batteries at the UE and power sensitivity of RF-DC circuits over a block fading channel. This algorithm is further expanded to multiple user (MU) systems. The main contributions of this paper can be summarized as follows.

- 1) We emphasize finite capacity batteries for the UL MIMO data transmission powered by RF WET, which represent

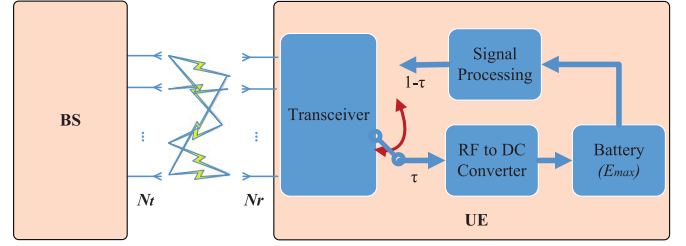


Fig. 1. MIMO system model with energy harvester at UE.

more practical scenarios and offer more flexibility of distributing the harvested energy between energy arrivals compared with existing works [16]–[18]. This system prevents the limitation of the environment and weather as renewable EH systems and prevents the artificially high performance arisen from ignoring the energy overflow as WET-enabled system with infinite capacity batteries.

- 2) We model the WET as a Bernoulli process with accurate probability  $p$  while taking into account the sensitivity of RF-DC circuits. We calculate the accurate WET probability  $p$  for given numbers of antennas at the BS and the UE.
- 3) We propose a low complexity online power and time allocation algorithm for WET-enabled MIMO UL communications. Specifically, power allocation consists of two steps, namely, constant fractional energy allocation and conventional water-filling methods. One-dimensional (1-D) search is used for time allocation.

*Notation:* All lower case and upper case boldface letters represent vectors and matrices, respectively. Let  $\text{tr}(\mathbf{X})$ ,  $\det(\mathbf{X})$ ,  $\mathbf{X}^{-1}$ , and  $\mathbf{X}^H$  denote the trace, determinant, inverse, and Hermitian of a symmetric matrix  $\mathbf{X}$ , respectively.  $\mathbb{C}^{x \times y}$  and  $\mathbb{R}^{x \times y}$  denote the set of complex and real matrices of size  $x \times y$ , respectively. We use  $\text{diag}(x_1, x_2, \dots, x_M)$  to stand for an  $M \times M$  diagonal matrix with diagonal elements  $x_1, x_2, \dots, x_M$ .  $\mathbb{E}(\cdot)$  denotes the statistical expectation,  $\text{Var}(\cdot)$  stands for the variance of the random variable, and  $\sim$  stands for “distributed as.”  $\mathbf{I}$  and  $\mathbf{0}$  denote an identity matrix and an all-zero vector with suitable dimensions, respectively. All the  $\log(\cdot)$  functions are of base 2 by default and  $\ln(\cdot)$  stands for the natural logarithm.

## II. SYSTEM MODEL AND PROBLEM FORMULATION

We consider a time division duplex MIMO system, as shown in Fig. 1, where the number of antennas equipped at the BS and at the UE is  $N_t$  and  $N_r$ , respectively. The UE uses the energy harvested from the BS WET to power its UL WIT, under the assumption that the BS and the UE are perfectly synchronized. The total capacity of battery storage in the UE is  $Q_{\max}$ .

A time slotted transmission pattern is considered, as shown in Fig. 2. Each slot has a constant duration  $T'$  and the total transmission period is  $T = NT'$ , where  $N$  denotes the total number of slots. Each slot consists of two phases, namely, the DL WET phase of duration  $\tau T'$ , and the UL WIT phase of duration  $(1 - \tau)T'$ , where  $0 \leq \tau \leq 1$ . The DL WET phase starts with several control frames, including the preamble, frame control

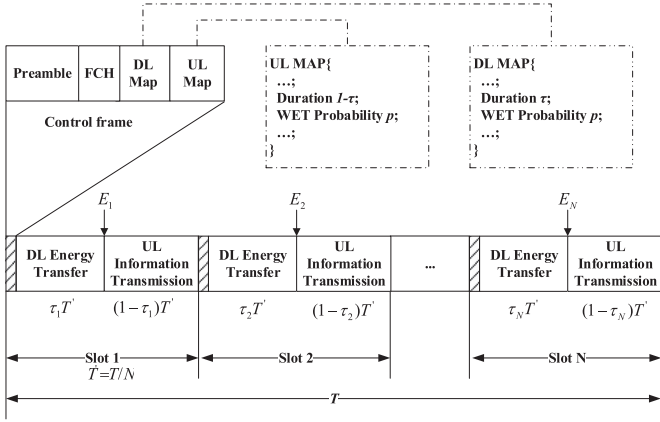


Fig. 2. Frame structure.

header, DL map, and UL map. These frames define transmission parameters, such as coding schemes, available resources, the duration of DL and UL transmission, and the WET probability (which is defined in the following). Then, the BS transmits energy to the UE through wireless energy beamforming. The received power level and the energy harvested at the UE in slot  $l$  ( $l = 1, \dots, N$ ) are denoted by  $P_l$  and  $E_l$ . It is worth noting that due to the power sensitivity of RF EH circuits, the UE cannot harvest any RF energy if the received signal power  $P_l$  is less than a certain level. In order to avoid wasting BS transmission energy, the BS will estimate the received power at the UE and will transfer energy to the UE if the estimated received power level  $P_l$  is larger than a certain threshold  $\alpha$  (e.g.,  $-25$  dBm). Thus, the WET follows a Bernoulli process with parameter  $p$ , which stands for the probability of delivering energy from BS. The UL WIT is powered by the energy stored in the UE batteries. The duration of each slot  $T'$  should be less than channel coherence time. For simplicity, we assume a normalized unit slot time in the sequel and that the harvested energy is stored in the battery first, and then used for UL information transmission, which is similar to the approaches used in [16]. Note that since the length of control frames is much smaller than that of DL WET and UL WIT, we ignore the time duration of control frames in the following analysis. We assume that the transmission distance between the BS and the UE is fixed throughout the transmission duration  $T$ . For a mobile UE, the BS updates the WET probability once the distance is changed, thus forming a new WET Bernoulli process with the updated parameter  $p$ .

Assuming the RF signals are transmitted on a single frequency band, we consider a block flat fading channel [23] (i.e., which means the channel remains constant in each slot). Denote  $\mathbf{H}_l \in \mathbb{C}^{N_t \times N_r}$  as the UL channel in the  $l$ th slot and we have

$$\mathbf{H}_l = \beta^{\frac{1}{2}} \mathbf{G}_l \quad (1)$$

where  $\mathbf{G}_l \in \mathbb{C}^{N_t \times N_r}$  denotes the Rayleigh fading coefficients with entries  $[G]_{mk} = g_{mk} \sim \mathcal{CN}(0, 1)$ , and  $\beta$  is the path loss between the BS and the UE. By exploiting the channel reciprocity, the DL transmission channel can be obtained as  $\mathbf{H}_l^H$ . For

simplicity, we assume causal channel state information (CSI) is available at both the BS and the UE.<sup>1</sup>

### A. DL Energy Transfer Phase

The BS delivers energy to the UE in the DL WET phase in each slot. Assuming that the ambient channel noise energy cannot be harvested. The received signal and the harvested energy at the UE in the  $l$ th slot are given by

$$y_l^{\text{DL}} = \mathbf{H}_l^H \mathbf{w}_l s_l + \mathbf{n}_l \quad (2)$$

$$E_l = \tau_l \eta_c P_l = \tau_l \eta_c \text{tr}(\mathbf{H}_l^H \mathbf{w}_l \mathbf{w}_l^H \mathbf{H}_l) \quad (3)$$

where  $\mathbf{n}_l \in \mathcal{CN}(\mathbf{0}, \sigma_1^2 \mathbf{I})$  is the  $N_r \times 1$  channel noise vector,  $\mathbf{w}_l$  is the  $N_t \times 1$  BS beamformer,  $\eta_c$  is the RF-DC conversion efficiency,  $P_l$  is the received power at the UE, and  $s_l$  is the random information carrying signal from the BS in slot  $l$  with zero mean and unit variance.

Denote  $M = \min(N_t, N_r)$  and  $B = \max(N_t, N_r)$ . Then, the reduced singular value decomposition of  $\mathbf{H}_l^H$  is given by  $\mathbf{H}_l^H = \mathbf{U}_{l,H} \mathbf{\Sigma}_{l,H}^{1/2} \mathbf{\Xi}_{l,H}^H$ , where  $\mathbf{U}_{l,H} \in \mathbb{C}^{N_r \times M}$  and  $\mathbf{\Xi}_{l,H} \in \mathbb{C}^{N_t \times M}$  (each consisting of orthogonal columns with unit norm), and  $\mathbf{\Sigma}_{l,H}^{1/2} \in \mathbb{C}^{M \times M}$  is a diagonal matrix containing the singular values of  $\mathbf{H}_l^H$ . Let  $\mathbf{W}_l = \mathbf{w}_l \mathbf{w}_l^H$  and  $P_{\max}$  be the maximum transmission power of the BS, then the optimal BS WET beamformer is given by [24]

$$\mathbf{W}_l = P_{\max} \xi_{l,1} \xi_{l,1}^H \quad (4)$$

where  $\xi_{l,1}$  is the first column of  $\mathbf{\Xi}_{l,H}$  and corresponds to the maximum singular value of  $\mathbf{H}_l^H$ . If there is only one antenna at the UE,  $\xi_{l,1} = \frac{\mathbf{h}_l}{\|\mathbf{h}_l\|}$ . Note that the maximum transmission power of the BS  $P_{\max}$  refers to the transmission power after power amplification through the amplifier. The UL transmission rate is directly related to  $P_{\max}$  rather than the power before amplification, so the energy consumption at the BS is omitted for the sake of simplicity.

Accordingly, the instantaneous received power at the UE in slot  $l$  can be obtained as follows:

$$\begin{aligned} P_l &= \text{tr}(\mathbf{H}_l^H \mathbf{w}_l \mathbf{w}_l^H \mathbf{H}_l) \\ &= P_{\max} \text{tr}\left(\mathbf{U}_{l,H} \mathbf{\Sigma}_{l,H}^{\frac{1}{2}} \mathbf{\Xi}_{l,H}^H \xi_{l,1} \xi_{l,1}^H \mathbf{\Xi}_{l,H} \mathbf{\Sigma}_{l,H}^{\frac{1}{2}} \mathbf{U}_{l,H}^H\right) \\ &\stackrel{(a)}{=} P_{\max} \text{tr}\left(\mathbf{\Sigma}_{l,H}^{\frac{1}{2}} \mathbf{e}_1 \mathbf{e}_1^H \mathbf{\Sigma}_{l,H}^{\frac{1}{2}}\right) \\ &= P_{\max} \lambda_{l,\max} \end{aligned} \quad (5)$$

where  $\mathbf{e}_1$  is the first column of the unit matrix  $\mathbf{I}$ , (a) holds because  $\text{tr}(\mathbf{A}\mathbf{B}) = \text{tr}(\mathbf{B}\mathbf{A})$  and  $\mathbf{U}^H \mathbf{U} = \mathbf{I}$ , and  $\lambda_{l,\max}$  is the maximum eigenvalue of  $\mathbf{H}_l \mathbf{H}_l^H$ .

<sup>1</sup>Due to the correlation between time slots, considering channel estimation errors in multiple-slot optimization will dramatically increase the complexity, as compared with single-slot optimization [16]. For tractability of analysis, we assume perfect CSI in this paper. The proposed algorithm can be extended to imperfect CSI scenarios by considering the ellipsoidal channel uncertainty model and worst case resource allocation criterion [22], which will be studied in our future work.

We can see from (5) that the instantaneous received power at the UE is only related to the maximum BS transmission power and the maximum singular value of the transmission channel. In the following, we will derive the energy transfer probability and the average received power based on (5).

The cumulative distribution function (CDF) of  $\lambda_{l,\max}$  is given by [25]

$$F_{\lambda_{l,\max}}(\lambda) = K \det(\mathbf{A}(\lambda)), \quad (6)$$

where  $K$  is defined as

$$K^{-1} = \prod_{i=1}^M (M-i)!(B-i)!, \quad (7)$$

and  $\mathbf{A}(\lambda) \in \mathbb{C}^{M \times M}$  is the Hankel matrix. The  $\{i, j\}$ th entity of  $\mathbf{A}(\lambda)$  is given by

$$\{\mathbf{A}\}_{i,j} = (B-M+i+j-2)! - \Gamma(B-M+i+j-1, \lambda), \quad (8)$$

where the upper incomplete gamma function  $\Gamma(s, x) = \int_x^\infty t^{s-1} e^{-t} dt$ .

The probability density function (PDF) of  $\lambda_{l,\max}$  can be obtained as

$$f_{\lambda_{l,\max}}(\lambda) = K \frac{d}{d\lambda} \det(\mathbf{A}(\lambda)). \quad (9)$$

PDF in (9) can be simplified as follows [26]:

$$f_{\lambda_{l,\max}}(\lambda) = K \sum_{k=1}^M \sum_{j=B-M}^{(B+M-2k)k} d_{k,j} \lambda^j e^{-k\lambda} \quad (10)$$

where the coefficients  $d_{k,j}$  in the DL WET phase in each slot can be obtained easily when  $N_r$  and  $N_t$  are fixed [26]. The corresponding CDF is given by

$$\begin{aligned} F_{\lambda_{l,\max}}(\lambda) &= \int_0^\lambda f_{\lambda_{l,\max}}(\lambda) d\lambda \\ &= K \sum_{k=1}^M \sum_{j=B-M}^{(B+M-2k)k} \frac{d_{k,j}}{k^{j+1}} \gamma(j+1, k\lambda) \end{aligned} \quad (11)$$

where the lower incomplete gamma function  $\gamma(s, x) = \int_0^x t^{s-1} e^{-t} dt$ .

Therefore, the average received power in slot  $l$  and the power transmitting probability  $p$  can be found as follows:

$$\begin{aligned} \bar{P}_l &= P_{\max} \beta \int_0^\infty \lambda f_{\lambda_{l,\max}}(\lambda) d\lambda \\ &= P_{\max} \beta K \sum_{k=1}^M \sum_{j=B-M}^{(B+M-2k)k} \frac{d_{k,j}}{k^{j+2}} \Gamma(j+2) \end{aligned} \quad (12)$$

$$\begin{aligned} p &= \Pr(P_{\max} \lambda > \alpha) \\ &= \int_{\frac{\alpha}{P_{\max}}}^\infty f_{\lambda_{l,\max}}(\lambda) d\lambda \\ &= K \sum_{k=1}^M \sum_{j=B-M}^{(B+M-2k)k} \frac{d_{k,j}}{k^{j+1}} \Gamma\left(j+1, \frac{\alpha k}{P_{\max}}\right) \end{aligned} \quad (13)$$

where the gamma function  $\Gamma(s) = \int_0^\infty x^{s-1} e^{-x} dx$ .

The above analysis is based on the assumption of constant RF-DC conversion efficiency, namely, a linear EH model is used. However, in practical scenarios, the rectifier of the EH receiver (circuit that converts RF to DC) is normally working on the nonlinear model with the increasing input power level. The above analysis is also suitable for the nonlinear case after some modifications. The nonlinear model defined in [27] is used in this paper. The received power is changed as follows:

$$P_l = \frac{1}{1-\Omega} \left| \frac{F}{1 + e^{-a(P_{\max} \lambda_{l,\max} - b)}} - F\Omega \right|, \quad (14)$$

where  $a$  and  $b$  are the parameters of the EH circuits,  $F$  denotes the maximum harvested power, and  $\Omega$  is given by

$$\Omega = \frac{1}{1 + e^{ab}} \in (0, 1). \quad (15)$$

Before calculating the energy transfer probability, we will first solve the inequality as follows:

$$\begin{aligned} &\frac{1}{1-\Omega} \left| \frac{F}{1 + e^{-a(P_{\max} \lambda_{l,\max} - b)}} - F\Omega \right| > \alpha \\ \Leftrightarrow &\begin{cases} \lambda_{l,\max} > -\frac{1}{ap} \ln \frac{D_1-1}{e^{ab}} & \text{if } a \geq 0 \\ \lambda_{l,\max} > -\frac{1}{ap} \ln \frac{D_2-1}{e^{ab}} & \text{if } a < 0 \end{cases}, \end{aligned} \quad (16)$$

where  $D_1 = \frac{1}{\frac{\alpha(1-\Omega)}{F} + \frac{1}{1+e^{ab}}}$  and  $D_2 = \frac{1}{\frac{1}{1+e^{ab}} - \frac{\alpha(1-\Omega)}{F}}$ . Next, by using the PDF of  $\lambda_{l,\max}$  in (9), we calculate the energy transfer probability in nonlinear model as follows:

$$\begin{aligned} p &= \begin{cases} \Pr\{\lambda_{l,\max} > -\frac{1}{ap} \ln \frac{D_1-1}{e^{ab}}\}, & \text{if } a \geq 0 \\ \Pr\{\lambda_{l,\max} > -\frac{1}{ap} \ln \frac{D_2-1}{e^{ab}}\}, & \text{if } a < 0 \end{cases} \\ &= \begin{cases} K \sum_{k=1}^M \sum_{j=B-M}^{(B+M-2k)k} \frac{d_{k,j}}{k^{j+1}} \Gamma\left(j+1, -\frac{1}{ap} \ln \frac{D_1-1}{e^{ab}}\right), & \text{if } a \geq 0 \\ K \sum_{k=1}^M \sum_{j=B-M}^{(B+M-2k)k} \frac{d_{k,j}}{k^{j+1}} \Gamma\left(j+1, -\frac{1}{ap} \ln \frac{D_2-1}{e^{ab}}\right), & \text{if } a < 0. \end{cases} \end{aligned} \quad (17)$$

Note that the fundamental features of the proposed algorithm (see Section III) are independent of the EH model (linear or nonlinear). In fact, there are many state-of-the-art techniques that can achieve a nearly constant conversion efficiency within a range of received power level [28]. Thus, the linear model can be used for the nonlinear case by choosing a specific received power range wherein the conversion efficiency remains nearly stable. The BS transmits energy only if the estimated received power level falls in this range. For the tractability of analysis, we only refer to the linear model unless stated otherwise. A comprehensive analysis of the RF-DC conversion efficiency model and its impact on the EH receiver are beyond the scope of this paper.

## B. UL Information Transmission Phase

In the UL WIT phase of each slot, the UE uses the harvested energy to power UL information transmission to the BS. The

received signal at the BS in the  $l$ th slot is given by

$$y_l^{\text{UL}} = \mathbf{H}_l \mathbf{v}_l \mathbf{s}_l' + \mathbf{z}_l \quad (18)$$

where  $\mathbf{v}_l$  is the  $N_r \times 1$  UL transmission beamforming weight vector,  $\mathbf{s}_l'$  denotes random information carrying signal with zero mean and unit variance, and the  $N_t \times 1$  noise vector  $\mathbf{z}_l \sim (\mathbf{0}, \sigma^2 \mathbf{I})$ .

The corresponding data rate (in bits/s/Hz) is given as

$$r_l = \log \det \left( \mathbf{I} + \frac{1}{\sigma^2} \mathbf{H}_l \mathbf{v}_l \mathbf{v}_l^H \mathbf{H}_l^H \right). \quad (19)$$

Let  $\mathbf{H}_l^H \mathbf{H}_l = \mathbf{\Upsilon}_l^H \mathbf{\Lambda}_l \mathbf{\Upsilon}_l$ , where  $\mathbf{\Lambda}_l = \text{diag}(\lambda_{l,1}, \dots, \lambda_{l,M}, 0, 0, \dots)$  contains the  $M$  eigenvalues of  $\mathbf{H}_l^H \mathbf{H}_l$ . Then, (19) can be rewritten as

$$r_l = \log \det \left( \mathbf{I} + \frac{1}{\sigma^2} \mathbf{\Lambda}_l^{1/2} \mathbf{S}_l \mathbf{\Lambda}_l^{1/2} \right) \quad (20)$$

where  $\mathbf{S}_l = \mathbf{\Upsilon}_l \mathbf{V}_l \mathbf{\Upsilon}_l^H$  and  $\mathbf{V}_l = \mathbf{v}_l \mathbf{v}_l^H$ . Since  $\mathbf{\Upsilon}_l$  is a unitary matrix,  $\text{tr}(\mathbf{S}_l) = \text{tr}(\mathbf{V}_l)$ .

The energy allocated for UL WIT in the  $l$ th slot is given by

$$q_l = (1 - \tau) \text{tr}(\mathbf{V}_l). \quad (21)$$

Let  $\eta_a$  and  $Q_l$  represent the efficiency of power amplifiers and the amount of energy available in the battery at slot  $l$ . The energy updating function is given as follows:

$$Q_l = \min \left( Q_{l-1} + E_l - \frac{q_{l-1}}{\eta_a}, Q_{\max} \right) \quad (22)$$

where  $\frac{q_{l-1}}{\eta_a}$  stands for the energy consumption of UL WIT.

There are two constraints in the UL WIT phase: the energy causality constraint and the battery storage constraint. Specifically, the energy causality constraint requires that the UL transmission can only use the energy harvested at the current and previous slots, i.e.

$$\sum_{i=0}^l \left[ E_i - \frac{(1 - \tau) \text{tr}(\mathbf{S}_i)}{\eta_a} \right] \geq 0. \quad (23)$$

The battery storage constraint indicates that the energy available at the UE cannot exceed the maximum battery capacity at any time, i.e.

$$\sum_{i=0}^{l+1} E_i - \sum_{i=0}^l \frac{(1 - \tau) \text{tr}(\mathbf{S}_i)}{\eta_a} \leq Q_{\max}. \quad (24)$$

### C. Problem Formulation

We consider both the offline scenario with noncasual CSI and the online scenario with casual CSI. Specifically, in the offline scenario, CSI in all the slots is known at the BS and the UE before the first slot starts, whereas the BS and the UE have only CSI of the current and past slots in the online scenario. The offline scenario is not practical, but it can be used to provide some insights into the design of online power and time allocation policy. In the following, optimization problems are formulated for these two different scenarios.

1) *Offline Scenario*: The offline scenario aims to maximize the number of information bits transmitted in  $N$  slots subject to the energy causality constraint, and the battery storage constraint. Using the optimal energy transmitting beamformer (4), the optimization problem is formulated as

$$\begin{aligned} \arg \max_{\mathbf{S}_l} \quad & \sum_{l=1}^N (1 - \tau_l) r_l \\ \text{s.t.} \quad & (23), (24). \end{aligned} \quad (25)$$

The offline power allocation for renewable enabled communications has been well studied [9], [10], and [12]. What is different in this paper is the need for time allocation.

Upon fixing the time allocation  $\tau_l = \tau$  for  $l = 1, \dots, N$ , we can solve problem (25) by using Lagrangian methods.

The Lagrangian function of (25) is

$$\begin{aligned} \mathcal{L}(\mathbf{S}, \alpha, \mu) = & \sum_{l=1}^N (1 - \tau) \log \det \left( \mathbf{I} + \frac{1}{\sigma^2} \mathbf{\Lambda}_l^{1/2} \mathbf{S}_l \mathbf{\Lambda}_l^{1/2} \right) \\ & - \sum_{l=1}^N \alpha_l \sum_{i=1}^l \left[ \frac{(1 - \tau)}{\eta_a} \text{tr}(\mathbf{S}_i) - E_i \right] \\ & - \sum_{l=1}^{N-1} \mu_l \left[ \sum_{i=1}^{l+1} E_i - \sum_{i=1}^l \frac{(1 - \tau)}{\eta_a} \text{tr}(\mathbf{S}_i) - Q_{\max} \right] \end{aligned} \quad (26)$$

where  $\alpha_l$  and  $\mu_l$  are the scalar Lagrange multipliers associated with (23) and (24), respectively.

Then, upon applying the Karush–Kuhn–Tucker conditions to (26) and setting  $\frac{\partial \mathcal{L}}{\partial \mathbf{S}_l} = 0$ , the optimal  $\mathbf{S}_l^*$  can be found as

$$\mathbf{S}_l^* = \frac{1}{\sum_{i=l}^N \alpha_i - \sum_{i=l}^{N-1} \mu_i} \mathbf{I} - \sigma^2 \mathbf{\Lambda}_l^{-1} \succeq 0. \quad (27)$$

From (27), we can see that  $\mathbf{S}_l^*$  is a diagonal matrix with the diagonal elements given by

$$S_{l,j}^* = \left[ \frac{1}{\sum_{i=l}^N \alpha_i - \sum_{i=l}^{N-1} \mu_i} - \frac{\sigma^2}{\lambda_j} \right]^+, \quad 1 \leq j \leq M \quad (28)$$

where  $[x]^+ = \max(0, x)$  and the water level is

$$v_l = \frac{1}{\sum_{i=l}^N \alpha_i - \sum_{i=l}^{N-1} \mu_i}. \quad (29)$$

We can observe from (27)–(29) that the water level is constant for different antennas in the same slot, because (29) is not related to  $j$ , the antenna element index. Thus, the power allocation for different antennas can be obtained by traditional water-filling algorithms. The spatial-temporal water-filling algorithm [12] can be used to obtain the optimal offline power. The time allocation can be found using 1-D search methods. Repeat power allocation and time allocation iteratively until certain stopping criterion is satisfied.

2) *Online Scenario*: Let  $r(q_l)$  denote the UL data rate in slot  $l$  as a function of the allocated energy  $q_l$  for UL transmission in slot  $l$ . Notice that  $q_l$  is a feasible online energy allocation policy

when it satisfies

$$0 \leq q_l \leq \eta_a Q_l \quad (30)$$

$$Q_{l+1} = \min \left( Q_l + E_{l+1} - \frac{q_l}{\eta_a}, Q_{\max} \right) \quad (31)$$

$$q_l = \phi(l, \{E_i\}_{i=1}^l) \quad (32)$$

where constraint (30) requires that the amount of energy allocated for UL WIT is no less than zero and must be no more than the energy available in the battery; (31) is the update function for the energy available in the battery; and (32) is the causality constraint, i.e., energy allocated in slot  $l$  only depends on the current and past WET process.

Let  $\mathcal{Q}$  denote the set of feasible online energy allocation policies. We define the online optimization problem as maximizing the average UL WIT data rate while satisfying constraints (30)–(32), i.e.

$$\arg \max_{q \in \mathcal{Q}, P_{l,j}, \tau_l} \lim_{N \rightarrow \infty} \frac{1}{N} \sum_{l=1}^N (1 - \tau_l) r(q_l), \quad (33)$$

where  $r(q_l) = \sum_{j=1}^M \log(1 + \frac{q_l}{N_r \sigma^2 (1 - \tau_l)} P_{l,j} \lambda_{l,j})$ , and  $P_{l,j}$  is the transmit power allocated on the  $j$ th subchannel in slot  $l$ , and we have  $S_{l,j}^* = \frac{q_l}{N_r \sigma^2 (1 - \tau_l)} P_{l,j}$ .

The optimal online time and power allocation policy can be solved by the dynamic programming (DP) method [29]. Specifically, at the beginning of the first slot, the BS recursively calculates the optimal time and power allocation policy via DP from the  $N$ th slot to the beginning slot. The optimal policy is a function of  $\mathbf{H}_l$  and available energy in the battery  $Q_l$ , and the BS records this function as a look-up table [11], [12]. At each slot, the BS can perform the optimal power allocation  $P_{l,j}$ ,  $j \in [1, N_r]$  and time allocation  $\tau_l$  based on the look-up table by updating the  $\mathbf{H}_l$  and  $Q_l$ . However, as the computational and storage requirements of DP increase exponentially with the number of state variables, DP is inefficient and unsuitable for online power and time allocation. In view of this, the comprehensive discussion on DP is beyond the scope of the current paper. We will propose a reduced-complexity online power and time allocation algorithm in the following section.

### III. ONLINE POWER AND TIME ALLOCATION

In this section, we propose an online power and time allocation algorithm to maximize the average data rate of UL WIT while satisfying constraints (30)–(32) for the online scenario with causal CSI available only.

#### A. Power Allocation

The online power allocation is performed in two steps in each slot. First, the optimal energy allocation is obtained by a constant fractional energy allocation policy. Second, the traditional water-filling algorithm is implemented to allocate the optimal power to each antenna at the UE.

In the following, we will first focus on the case when  $\tau_l \alpha \eta_a \geq Q_{\max}$ , i.e., the battery capacity  $Q_{\max}$  is no larger than the amount of energy that can be harvested by the UE in slot  $l$ .

In this case, if the BS performs WET, the battery will be charged to full, and the energy arrival process only depends on the battery size and the energy transfer probability  $p$ . If we define the period between two adjacent energy arrivals as an epoch and each epoch is independent, then the energy arrival process is a Bernoulli process

$$E_l = \begin{cases} Q_{\max} & \text{w.p. } p \\ 0 & \text{w.p. } 1 - p \end{cases} \quad (34)$$

where w.p. means “with probability,” and  $p$  is given in (13).

Therefore, when  $\tau_l \alpha \eta_a \geq Q_{\max}$ , the battery is fully charged, and the power allocation policy is only dependent on the number of slots from the last energy arrival slot to the current slot. Specifically, let  $q_l = \hat{q}_i$ , where  $i = l - \max\{t | t \leq l, E_t = Q_{\max}\}$ . The corresponding constraints on  $\hat{q}_i$  are given as follows:

$$\hat{q}_i \geq 0 \quad (35)$$

$$\sum_{i=0}^{\infty} \hat{q}_i \leq Q_{\max}. \quad (36)$$

Following (35) and (36),  $q_l$  clearly satisfies (30) and (31). Since  $q_l$  relies on the current and past slots’ energy arrivals, it also satisfies (32). Accordingly, the power allocation policy is given by

$$\hat{q}_i = p(1 - p)^i \eta_a^{i+1} Q_{\max}. \quad (37)$$

Since the energy arrival process follows the Bernoulli process with parameter  $p$ , the energy arriving interval time is a geometrically distributed random with a mean value  $1/p$ . Therefore, the expected time interval between two adjacent energy arrivals is  $1/p$ . If in slot  $l$ , the UE knows exactly the number of slots  $c$  that it has to wait until the next energy arrival, then the optimal energy allocation policy can be obtained as  $\eta_a Q_l / c$ , where  $Q_l$  is the amount of available energy stored in the batteries in slot  $l$ . This is because uniformly distributing the energy between energy arrivals maximizes the data rate [9]. Since there is no instantaneous knowledge about the next energy arrival time in the online scenario, the expected time interval between two adjacent energy arrivals  $1/p$  is used. Thus, a fraction  $p$  of the currently available energy is used for the UL WIT in the current slot.

For the case of  $\tau_l \alpha \eta_a < Q_{\max}$ , we can use the same method as for the case of  $\tau_l \alpha \eta_a \geq Q_{\max}$ , except for replacing  $Q_{\max}$  with the available energy in the battery. Let  $q_l = \hat{q}_i$ , where  $i = l - \max\{t | t \leq l, E_t > 0\}$ , then the power allocation policy for  $\tau_l \alpha \eta_a < Q_{\max}$  is given by

$$\hat{q}_i = p(1 - p)^i \eta_a^{i+1} Q_{i'} \quad (38)$$

where  $i' = \max\{t | t \leq l, E_t > 0\}$ . The power allocation in (38) can also be applied to the case of  $\tau_l \alpha \eta_a \geq Q_{\max}$  because  $Q_{i'} = Q_{\max}$  in that case.

After getting the energy allocated for the UL WIT in slot  $l$ , the corresponding average transmission power is  $\frac{q_l}{1 - \tau_l}$ . Then, the power allocated to each antenna of the UE is determined

using the traditional water-filling algorithm [30] as follows:

$$P_{l,j} = \left[ \nu_l - \frac{N_r(1-\tau_l)\sigma^2}{q_l} \cdot \frac{1}{\lambda_{l,j}} \right]^+. \quad (39)$$

Since  $S_{l,j}^* = \frac{q_l}{N_r\sigma^2(1-\tau_l)}P_{l,j}$ , we have  $\nu_l = \frac{N_r\sigma^2(1-\tau_l)}{q_l}\nu_l$ , where  $\nu_l$  is defined in (29).

### B. Time Allocation

In this section, we will study the optimal time allocation policy. Because  $Q_l \in [0, Q_{\max}]$ , the allocated time  $\tau_l$  must satisfy the following:

$$0 \leq \tau_l < \delta \quad (40)$$

where  $\delta = \min\left(1, \frac{Q_{\max} - (Q_{l-1} - \frac{q_{l-1}}{a})}{P_l}\right)$  is a function of  $\tau_{l-1}$ . Assume that  $q_l$ ,  $Q_l$ , and  $P_{l,j}$  are all functions of  $\tau_l$  and can be written as  $q_l(\tau_l)$ ,  $Q_l(\tau_l)$ , and  $P_{l,j}(\tau_l)$ , respectively. The optimal time allocation policy can be obtained by solving the following optimization problem:

$$\arg \max_{\tau_l} (1-\tau_l) \sum_{j=1}^M \log \left( 1 + \frac{q_l(\tau_l)P_{l,j}(\tau_l)\lambda_{l,j}}{N_r\sigma^2(1-\tau_l)} \right) \quad (41)$$

$$\text{s.t. } 0 \leq \tau_l < \delta(\tau_{l-1}).$$

In the following, we show that the optimization problem in (41) is convex. Defining  $\tilde{r}_{l,j}(\tau_l) = (1-\tau_l) \log\left(1 + \frac{q_l(\tau_l)}{N_r\sigma^2(1-\tau_l)}P_{l,j}(\tau_l)\lambda_{l,j}\right)$  and substituting (39) into it, we have

$$\tilde{r}_{l,j}(\tau_l) = (1-\tau_l) \log \left( 1 + \left( \frac{C_1\tau_l + C_2}{1-\tau_l} - \frac{1}{\lambda_{l,j}} \right) \lambda_{l,j} \right) \quad (42)$$

where  $C_1 = \frac{pP_l}{N_r\sigma^2}$  and  $C_2 = \frac{p(Q_{l-1} - q_{l-1})}{N_r\sigma^2}$ . The first-order and second-order derivatives of  $\tilde{r}_{l,j}(\tau_l)$  are given as follows:

$$\frac{d\tilde{r}_{l,j}(\tau_l)}{d\tau_l} = \frac{C_1 + C_2 - (C_2 + C_1\tau_l) \ln \left( \frac{\lambda_{l,j}(C_2 + C_1\tau_l)}{1-\tau_l} \right)}{\ln 2 \cdot (C_2 + C_1\tau_l)} \quad (43)$$

$$\frac{d^2\tilde{r}_{l,j}(\tau_l)}{d\tau_l^2} = \frac{(C_1 + C_2)^2}{(\tau_l - 1)(C_2 + C_1\tau_l)^2 \ln 2}. \quad (44)$$

We can see that  $\tilde{r}_{l,j}(\tau_l)$  is a concave function because  $\frac{d^2\tilde{r}_{l,j}(\tau_l)}{d\tau_l^2} < 0$  for  $0 \leq \tau_l \leq \delta$ . Thus, the problem (41) is a convex problem and can be readily solved by using 1-D search methods [31].

### C. Power and Time Allocation Algorithm

In this section, we propose a simple online power and time allocation algorithm for UL WIT powered by DL WET. The proposed algorithm includes an outer layer and an inner layer. The outer layer is to get the optimal time allocation  $\tau_l$  by solving problem (41) with the aid of the *golden section search method* [31]. In the inner layer, a fraction  $p$  of the available energy  $Q_l$  is allocated for UL WIT in slot  $l$ , and the power level  $P_{l,j}$  is allocated to the  $j$ th antenna at the UE following the water-filling algorithm in (39). It is worth noting that if no energy is received in slot  $l$ , then the algorithm sets  $\tau_l = \tau_{l-1}$ . The proposed online

---

### Algorithm 1: Online Power and Time Allocation Algorithm.

---

**Input:**  $\mathbf{H}_l, P_{\max}, Q_{l-1}, q_{l-1}$

**Output:** Optimal power and time allocations  $P_{l,j}, \tau_l$

- 1: **if** No energy is received in slot  $l$  **then**
  - 2:   Set  $\tau_l = \tau_{l-1}$ ;
  - 3:   Get power allocation by  $[P_{l,j}(\tau_l)]_{j=1}^M = \Psi(\tau_l)$ ;
  - 4: **else**
  - 5:   Set  $[a, b] = [0, \delta]$  and initial time allocation points  $c$  and  $d$ ;
  - 6:   **loop**
  - 7:     Get  $[P_{l,j}(c)]_{j=1}^M = \Psi(c)$  and  $[P_{l,j}(d)]_{j=1}^M = \Psi(d)$ ;
  - 8:     Get  $r_l(c)$  and  $r_l(d)$  by  $r_l(\tau_l) = \sum_{j=1}^M r_{l,j}(\tau_l)$  according to  $[P_{l,j}(c)]_{j=1}^M, [P_{l,j}(d)]_{j=1}^M$ ;
  - 9:     Compare  $r_l(c)$  and  $r_l(d)$  and update  $a, b$  according to the *golden section search method* [31].
  - 10:    **if** certain stopping criterion is satisfied **then**
  - 11:      $\tau_l = \frac{b-a}{2}$  and  $[P_{l,j}(\tau)]_{j=1}^M = \Psi(\tau)$ ;
  - 12:     Break;
  - 13:    **end if**
  - 14:    **end loop**
  - 15: **end if**
- 

power and time allocation algorithm is presented in Algorithm 1, where the inner layer is denoted as  $[P_{l,j}(\tau_l)]_{j=1}^M = \Psi(\tau_l)$

In general, the proposed online power and time allocation algorithm can be implemented in slot  $l$  as follows. First, the BS calculates the WET probability  $p$ , power allocation  $P_{l,j}$ , and time allocation  $\tau_l$  following Algorithm 1. Second, the BS broadcasts the values of  $p$  and  $\tau_l$  to the UE via control frames. Finally, the UE calculates power allocation according to  $p, \tau_l$  by allocating a fraction  $p$  of the available energy in the battery and traditional water-filling algorithms.

The proposed algorithm actually always converges to the solution. First, the time allocation has been proven to be a convex problem and can always be solved by 1-D methods. Second, the power allocation is composed of the  $p$ -fraction of available energy and the traditional water-filling method, both of which are convergent.

The complexity of the outer layer is  $O(\log(\frac{1}{\varepsilon}))$ , where  $\varepsilon$  is the precision of the optimal time allocation. The computation of the inner layer includes two parts:  $p$ -fraction of available energy, and the traditional water-filling algorithm. The former involves only 1 multiplication, while the complexity of the latter is  $O(M^2)$ , where  $M = \min(N_t, N_r)$ . In this case, the total complexity of the inner layer is  $O(M^2 + 1) \approx O(M^2)$ . Thus, the computational complexity of the proposed algorithm is  $O(M^2 \log(\frac{1}{\varepsilon}))$ . Note that the complexity of the traditional water filling can be reduced to  $O(M)$  through some improved water-filling algorithms [34]. Accordingly, the total computational complexity of the proposed algorithm is  $O(M \log(\frac{1}{\varepsilon}))$ .

#### IV. ONLINE SOLUTION FOR MU SYSTEMS

In this section, we expand our proposed algorithm to MU systems. Since this paper emphasizes on the online algorithm for a point-to-point link, we only provide two simple extension methods for the MU system. More complex problems, such as double near-far problems, user fairness, optimal power allocation, and energy beamforming at the BS for diverse users, are also important for MU systems and remain the future works.

##### A. Time Division Method

The system includes a BS equipped with  $N_t$  antennas and  $U$  UEs each equipped with  $N_r$  antennas. Each slot is divided into  $U$  parts equally, and each part serves one UE. Thus, the rate performance among UEs is independent and no MU interference is caused. Therefore, for the  $u$ th UE in the  $l$ th slot, the online solution can be obtained by solving the following problem:

$$\begin{aligned} \arg \max_{P_{l,u,j}, \tau_{l,u}} \quad & \lim_{N \rightarrow \infty} \frac{1}{N} \sum_{l=1}^N \frac{1}{U} (1 - \tau_{l,u}) r(q_{l,u}) \\ \text{s.t.} \quad & 0 \leq q_{l,u} \leq \eta_a Q_{l,u} \\ & Q_{l+1,u} = \min \left( Q_{l,u} + E_{l+1,u} - \frac{q_{l,u}}{\eta_a}, Q_{\max,u} \right) \\ & q_{l,u} = \phi(l, u, \{E_{i,u}\}_{i=1}^l). \end{aligned} \quad (45)$$

There is not much difference between (45) and (33), so we can use the method in the previous section to solve this problem.

##### B. Space Division Method

The system includes one BS with  $N_t$  antennas and  $U$  UEs with single antenna. For simplicity, we assume that the WET stage for all UEs in the  $l$ th slot stands for  $\tau_l \in (0, 1)$ , the BS equally allocates power for UEs, and the distance between the BS and each UE is equal. Denote  $\beta$  and  $\mathbf{h}_u \in \mathbb{C}^{N_t \times 1}$  are the path loss and the UL channel between the BS and the  $u$ th UE, respectively. The optimal power allocation and the optimal precoding design at the BS remain future works. Let  $\mathbf{H}_l = [\mathbf{h}_{l,1}, \mathbf{h}_{l,2}, \dots, \mathbf{h}_{l,U}]$  be the UL channel between the BS and  $U$  UEs. Assume entities of  $\mathbf{h}_{l,u}$  follow  $\mathcal{CN}(0, 1)$ . In the DL WET phase, we adopt maximum ratio transmission precoding at the BS due to the low computational complexity, which is given by

$$\mathbf{f}_{l,u} = \frac{\mathbf{h}_{l,u}}{\|\mathbf{h}_{l,u}\|_2}. \quad (46)$$

The received signal at the  $u$ th UE in the  $l$ th slot is given by

$$\mathbf{y}_{l,u}^{\text{DL}} = \sqrt{\bar{P}\beta} \mathbf{h}_{l,u}^H \mathbf{f}_{l,u} + \sqrt{\bar{P}\beta} \sum_{j=1, j \neq u}^U \mathbf{h}_{l,u}^H \mathbf{f}_{l,j} + \mathbf{n}_{l,j} \quad (47)$$

where  $\bar{P} = \frac{P_{\max}}{U}$ . Therefore, the received power of the  $u$ th UE is

$$P_{l,u}^{\text{DL}} = \bar{P}\beta |\mathbf{h}_{l,u}^H \mathbf{f}_{l,u}|^2 + \bar{P}\beta \sum_{j=1, j \neq u}^U |\mathbf{h}_{l,u}^H \mathbf{f}_{l,j}|^2. \quad (48)$$

In the following, we calculate the WET probability. Define

$$X_u = \bar{P}\beta |\mathbf{h}_{l,u}^H \mathbf{f}_{l,u}|^2 \quad (49)$$

and

$$Y_u = \bar{P}\beta \sum_{j=1, j \neq u}^U |\mathbf{h}_{l,u}^H \mathbf{f}_{l,j}|^2. \quad (50)$$

Since  $h_{l,u,j}^H \sim \mathcal{CN}(0, 1), \forall 1 \leq j \leq N_t$ , we have [32]

$$X_u \sim \text{Ga}(N_t, \bar{P}\beta) \quad (51)$$

where  $\text{Ga}(k, b)$  denotes gamma distribution with shape parameter  $k$  and scale parameter  $b$ . The PDF of gamma distribution is  $f(x) = \frac{1}{\Gamma(k)b^k} x^{k-1} e^{-\frac{x}{b}}$ .

According to the second-order Gamma approximation in [33],  $Y_u$  follows the gamma distribution  $\text{Ga}(A1, A2)$ , and the parameters  $A1$  and  $A2$  are given by

$$A1 = \frac{(\mathbb{E}(X_u))^2}{\text{Var}(Y_u)} = U - 1, \quad (52)$$

and

$$A2 = \frac{\text{Var}(X_u)}{(\mathbb{E}(Y_u))} = \bar{P}\beta. \quad (53)$$

Thus, the received power follows gamma distribution, which is given by

$$P_{l,u} \sim \text{Ga}(N_t + U - 1, \bar{P}\beta), \quad (54)$$

and the WET probability can be obtained by

$$\begin{aligned} p &= \Pr(P_{l,u} > \alpha_u) \\ &= \int_{\alpha_u}^{\infty} \frac{1}{\Gamma(N_t + U - 1) \bar{P}\beta^{N_t + U - 1}} x^{N_t + U - 2} e^{-\frac{x}{\bar{P}\beta}} dx. \end{aligned} \quad (55)$$

In the UL WIT phase, the received signal associated with the  $u$ th user at the BS is given by

$$\mathbf{y}_{l,u}^{\text{UL}} = \sqrt{P_{l,u}^{\text{UL}} \beta} \mathbf{h}_{l,u} s_u + \sum_{j=1, j \neq u}^U \sqrt{P_{l,j}^{\text{UL}} \beta} \mathbf{h}_{l,u} s_j + \mathbf{n}_{l,u} \quad (56)$$

where  $P_{l,u}^{\text{UL}}$  is the UL transmit power of the  $u$ th UE in the  $l$ th slot.

The MU interference can be mitigated by signal detector  $\mathbf{W}_l = [\mathbf{w}_{l,1}, \mathbf{w}_{l,2}, \dots, \mathbf{w}_{l,U}]$  at the BS, such as zero forcing (ZF) and maximum ratio combine (MRC) detectors

$$\mathbf{W}_l = \begin{cases} \mathbf{H}_l (\mathbf{H}_l^H \mathbf{H}_l)^{-1} & \text{for ZF} \\ \mathbf{H}_l^H & \text{for MRC} \end{cases} \quad (57)$$

After signal detecting, the detected signal associated with the  $u$ th UE is

$$\begin{aligned} \hat{s}_{l,u}^{\text{UL}} &= \sqrt{P_{l,u}^{\text{UL}} \beta} \mathbf{w}_{l,u}^H \mathbf{h}_{l,u} s_u \\ &+ \sum_{j=1, j \neq u}^U \sqrt{P_{l,j}^{\text{UL}} \beta} \mathbf{w}_{l,j}^H \mathbf{h}_{l,u} s_j + \mathbf{w}_{l,u}^H \mathbf{n}_{l,u}. \end{aligned} \quad (58)$$

Thus, the UL rate of the  $u$ th UE can be calculated by

$$r_{l,u} = \log \left( 1 + \frac{P_{l,u}^{\text{UL}} \beta |\mathbf{w}_{l,u}^H \mathbf{h}_{l,u}|^2}{\sigma^2 |\mathbf{w}_{l,u}^H \mathbf{w}_{l,u}| + \sum_{j=1, j \neq u}^U P_{l,j}^{\text{UL}} \beta |\mathbf{w}_{l,j}^H \mathbf{h}_{l,u}|^2} \right). \quad (59)$$

Therefore, the online solution can be obtained by solving the following problem:

$$\begin{aligned} \arg \max_{P_{l,u}, \tau_l} \quad & \lim_{N \rightarrow \infty} \frac{1}{N} \sum_{l=1}^N \sum_{u=1}^U (1 - \tau_l) r_{l,u} \\ \text{s.t.} \quad & 0 \leq q_{l,u} \leq \eta_a Q_{l,u} \\ & Q_{l+1,u} = \min \left( Q_{l,u} + E_{l+1,u} - \frac{q_{l,u}}{\eta_a}, Q_{\max,u} \right) \\ & q_{l,u} = \phi(l, u, \{E_{i,u}\}_{i=1}^l) \end{aligned} \quad (60)$$

where  $q_{l,u} = \tau_l P_{l,u}^{\text{UL}}$ . This problem is similar to (33) and can be solved by similar methods of Algorithm 1.

Note that in this section, we focus on single-cell MU-MIMO transmissions and UL intracell interference cancellation. Intercell interference (i.e., MU interference among adjacent cells) can be eliminated by UL coordinated multipoint (CoMP) reception [35], where multiBSs jointly detect the received MU signals and eliminate the intercell MU interference. Our proposed algorithm is compatible with UL CoMP reception.

## V. NUMERICAL RESULTS

To testify the performance of the proposed algorithm, numerical results are presented in this section. Throughout the simulations, the following settings are used unless stated otherwise. The BS and the UE are equipped with three and two antennas, respectively. The BS has the unit power budget ( $P_{\max} = 1$  W). We set the bandwidth as 100 KHz and the density of noise as  $-170$  dBm/Hz, so the power of the channel noise is  $\sigma_1^2 = \sigma^2 = -120$  dBm [16]. Let path loss follow the indoor office scenario in ‘‘WINNER II channel models’’ [36], where  $\beta(\text{dB}) = 20 \log_{10}(D[m]) + 51.4 + 20 \log_{10}(\frac{f_c[\text{GHz}]}{5})$ , with the propagation distance  $D = 10$  m and the carrier frequency  $f_c = 2.6$  GHz. The battery storage capacity  $Q_{\max} = 5 \times 10^{-6}$  J, the RF-DC conversion efficiency  $\eta_c = 0.4$ , and the power sensitivity of EH circuits  $\alpha = 3 \mu\text{W}$ .<sup>2</sup>

For performance comparison with the proposed algorithm, we include in the simulations the following existing power allocation algorithms: the FP allocation algorithm [14], the constant water level (CWL) algorithm [10], [12], and the energy adaptive (EA) algorithm [10], [12]. Combining with fixed or adaptive time allocation, we will testify six online power and time allocation policies, namely, FP, CWL, and EA with adaptive or fixed time allocation policies, respectively. For simplicity, we add

<sup>2</sup>The RF-DC conversion efficiency, the carrier frequency, and the power sensitivity of EH circuits can take different values ranging from 10% to 90%, from 450 MHz to 5.8 GHz, and from  $-40$  dBm ( $0.1 \mu\text{W}$ ) to  $-10$  dBm ( $10 \mu\text{W}$ ), respectively, as given in [4, Table III] and in [28] and [37].

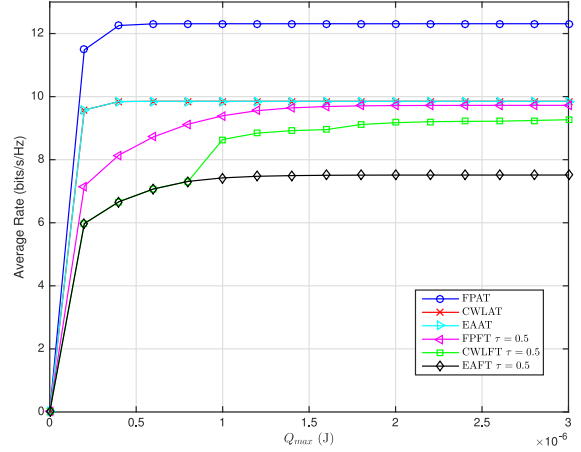


Fig. 3. Average rate versus UE battery capacity.

AT or FT at the end of each algorithm abbreviation to denote whether it is with adaptive or fixed time allocation, respectively. Therefore, the proposed algorithm is denoted as FPAT. Note that the solution in [14] is originally provided for renewable energy powered systems and cannot directly be used for the system model of this paper. We compare our proposed algorithm with a modified version of the solution in [14], called FPFT, which incorporates a MIMO channel, energy beamforming, calculation of energy transfer probability, estimation of received power level, and water-filling power allocation. Algorithms proposed in [16] and [17] allocated all the harvested energy to the UL WIT in the current slot, and thus belong to EA algorithms.

Fig. 3 demonstrates the average UL WIT rates versus the UE battery size  $Q_{\max}$ , where  $\tau = 0.5$  for fixed time allocation. We can see that the average rate first increases dramatically with  $Q_{\max}$  and then converges to a constant value for large values of  $Q_{\max}$ . This is because a larger battery size enables more energy stored into the battery and can thus support a higher data rate, but when the battery size gets larger than its received energy, the data rate becomes independent of the battery size. The proposed FPAT algorithm shows the highest data rate among all these algorithms. With adaptive time allocation, CWLAT allocates all the available energy in the battery to the current slot, thereby experiencing the same performance as EAAT. The battery with small capacity (e.g.,  $Q_{\max} \leq 0.7 \mu\text{W}$ ) will be fully charged once there is energy received. In this case, the product of average DL received power and fixed WET time duration is likely to be larger than the battery’s capacity, so CWLFT shows the same rate performance as EAFT. However, with the increasing battery capacity, it has been shown that CWLFT outperforms EAFT in terms of average data rate [10]. Therefore, there is an abrupt increase at about  $Q_{\max} = 0.7 \mu\text{W}$  for the CWLFT.

Fig. 4 shows the average rate (the left vertical axis) versus the EH power sensitivity of RF-DC circuits, where  $\tau = 0.5$  for fixed time allocation. The dash line denotes the energy transfer probability (the right vertical axis). We can see that when  $\alpha$  increases from 0 to  $10^{-5}$  W, the energy transfer probability decreases from 1 toward 0. The average rate of each considered algorithm decreases with  $\alpha$ , because the UE harvested energy decreases with the worsening sensitivity. The proposed FPAT

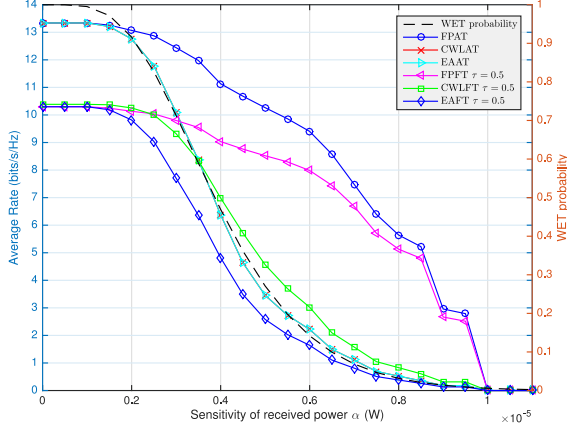


Fig. 4. Average rate versus EH power sensitivity.

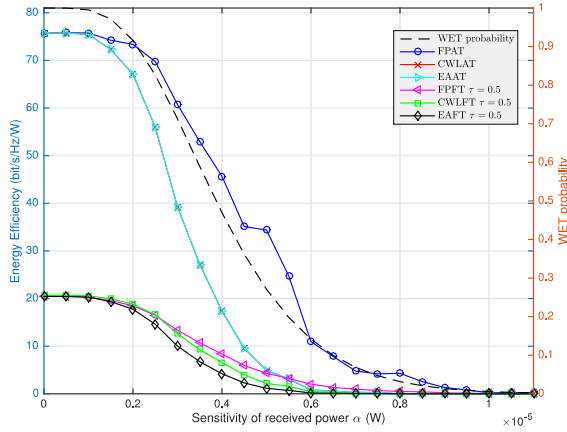


Fig. 5. Average energy efficiency versus EH power sensitivity.

algorithm has a higher rate than all the other algorithms for  $\alpha$  ranging from about 2 to 10  $\mu\text{W}$ . FPAT has the same performance as CWLAT and EAAT for very small values of  $\alpha$ , because the energy transfer probability is closed to 1 in that case.

Fig. 5 shows the average energy efficiency versus the EH power sensitivity of RF-DC circuits. The average energy efficiency is defined as

$$\eta_e = \lim_{N \rightarrow \infty} \frac{1}{N} \sum_{l=1}^N \frac{(1 - \tau_l)r(q_l)}{P_{\max} \tau_l} \quad (61)$$

where  $P_{\max} \tau_l$  is the energy cost at BS in slot  $l$ . We can see that the energy efficiency of the proposed FPAT algorithm is much higher than all the other considered algorithms, because of the adaptive time allocation and the high rate performance of the proposed algorithm.

Fig. 6 depicts the outage probabilities versus the EH power sensitivity of the RF-DC circuits, where the threshold of received SNR at the BS is 3 dB. We can see that the proposed FPAT algorithm shows the best outage performance among all these algorithms. Since CWLAT, EAAT, and EAFT will allocate all the available energy in the UE battery for the current slot UL transmission, resulting in energy shortage when no energy is received in some slots, they have the highest outage probability.

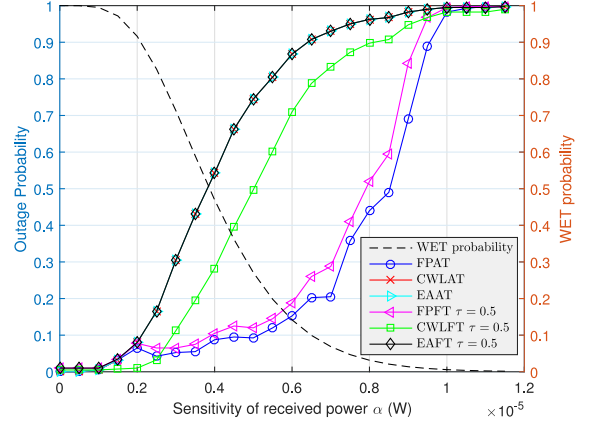


Fig. 6. Outage probability versus EH power sensitivity (threshold 3 dB).

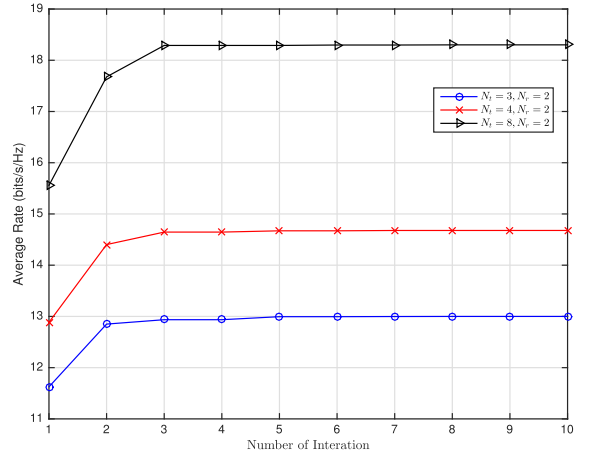


Fig. 7. Average iteration numbers.

Because CWLFT does not take energy shortage into consideration, its outage probability is also very high. Fig. 7 shows the average number of iterations to obtain the solution under various number of transmission antennas (three, four, and eight, respectively). The precision of the optimal time allocation is 0.001. We can find that the proposed algorithm can obtain solutions within four iterations.

Fig. 8(a) and (b) compares the average rate of the proposed FPAT and FPFT with different values of  $\tau$  versus the RF-DC circuit power sensitivity and for different noise power  $\sigma^2$ . For each considered noise power value and  $\alpha$ , the proposed FPAT algorithm always achieves the highest average rate among all the considered algorithms. The average rate of FPFT varies with different values of  $\tau$  and  $\sigma^2$ . For  $\sigma^2 = 10^{-15}$  W, FPFT with  $\tau = 0.3$  achieves an average rate very close to that of FPAT, while FPFT with  $\tau = 0.5$  achieves an average rate very close to that of FPAT for  $\sigma^2 = 10^{-12}$  W. This indicates that a fixed time allocation cannot always maximize the average data rate when the communication environment changes, whereas the proposed FPAT can adaptively allocate BS WET time and thereby get the maximum average data rate.

Fig. 9 shows the average rate performance of MU systems by the space division method versus EH power sensitivity of the RF-DC circuits. There is one BS equipped with three antennas

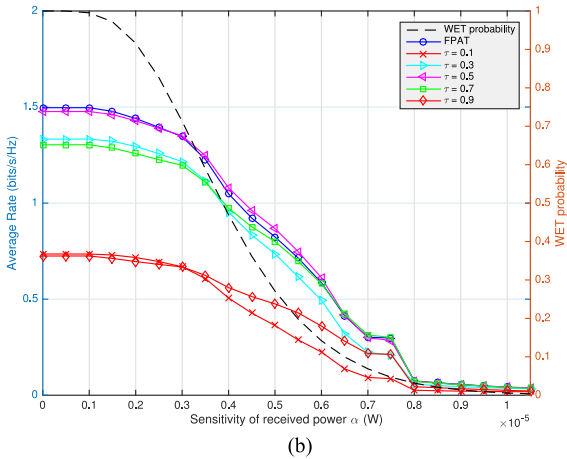
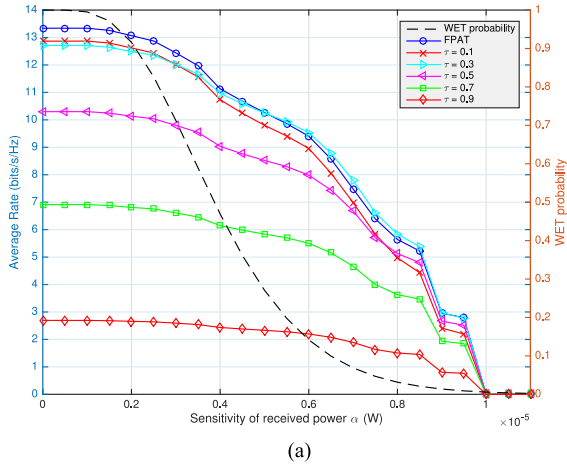


Fig. 8. Rate performance comparison between adaptive time and fixed time allocation. (a)  $\sigma^2 = 10^{-15}$  W. (b)  $\sigma^2 = 10^{-12}$  W.

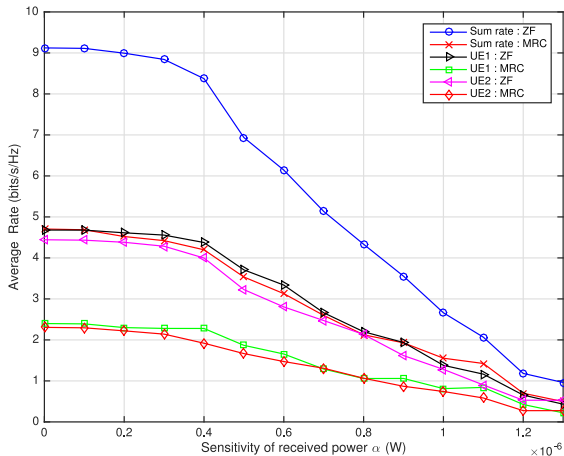


Fig. 9. Average rate versus EH power sensitivity for MU systems by the space division method.

and two UEs each equipped with single antenna. The distance between each UE and the BS is 10 m. ZF and MRC detectors are used to mitigate the MU interference. The average rate of using ZF detectors outperforms that of using MRC detectors.

## VI. CONCLUSION

In this paper, we have studied the power and time allocation for MIMO UL transmission powered by RF WET with finite capacity batteries at the UE. After calculating the probability of energy being transmitted from the BS to the UE, we propose a simple online algorithm with a fraction  $p$  of available energy allocated for UL WIT and adaptive time allocation in each slot. The numerical results have shown that the proposed FPAT algorithm achieves much better performance (i.e., higher average data rate, higher energy efficiency, and lower outage probability) as compared to the existing algorithms. We also provide two methods to extend the proposed algorithm to MU systems with the consideration of MU interference.

## REFERENCES

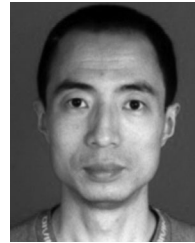
- [1] J. A. Paradiso and T. Starner, "Energy scavenging for mobile and wireless electronics," *IEEE Pervasive Comput.*, vol. 4, no. 1, pp. 18–27, Jan.–Mar. 2005.
- [2] Z. Ding *et al.*, "Application of smart antenna technologies in simultaneous wireless information and power transfer," *IEEE Commun. Mag.*, vol. 53, no. 4, pp. 86–93, Apr. 2015.
- [3] X. Chen, Z. Zhang, H.-H. Chen, and H. Zhang, "Enhancing wireless information and power transfer by exploiting multi-antenna techniques," *IEEE Commun. Mag.*, vol. 53, no. 4, pp. 133–141, Apr. 2015.
- [4] X. Lu, P. Wang, D. Niyato, D. I. Kim, and Z. Han, "Wireless networks with RF energy harvesting: A contemporary survey," *IEEE Commun. Surveys Tuts.*, vol. 17, no. 2, pp. 757–789, Apr.–Jun. 2015.
- [5] J. O. Mur-Miranda *et al.*, "Wireless power transfer using weakly coupled magnetostatic resonators," in *Proc. IEEE Energy Convers. Congr. Expo.*, Atlanta, GA, USA, Sep. 2010, pp. 4179–4186.
- [6] G. Papotto, F. Carrara, A. Finocchiaro, and G. Palmisano, "A 90-nm CMOS 5-Mbps crystal-less RF-powered transceiver for wireless sensor network nodes," *IEEE J. Solid-State Circuits*, vol. 49, no. 2, pp. 335–346, Feb. 2014.
- [7] N. Barroca *et al.*, "Antennas and circuits for ambient RF energy harvesting in wireless body area networks," in *Proc. IEEE Int. Symp. Pers., Indoor, Mobile Radio Commun.*, London, U.K., Sep. 2013, pp. 532–537.
- [8] U. Olgun, C. C. Chen, and J. L. Volakis, "Low-profile planar rectenna for batteryless RFID sensors," in *Proc. IEEE Antennas Propag. Soc. Int. Symp.*, Toronto, ON, Canada, Jun. 2010, pp. 1–4.
- [9] J. Yang and S. Ulukus, "Optimal packet scheduling in an energy harvesting communication system," *IEEE Trans. Commun.*, vol. 60, no. 1, pp. 220–230, Jan. 2012.
- [10] O. Ozel, K. Tutuncuoglu, J. Yang, S. Ulukus, and A. Yener, "Transmission with energy harvesting nodes in fading wireless channels: Optimal policies," *IEEE J. Sel. Areas Commun.*, vol. 29, no. 8, pp. 1732–1743, Sep. 2011.
- [11] I. Ahmed, A. Ikhlef, D. W. K. Ng, and R. Schober, "Power allocation for an energy harvesting transmitter with hybrid energy sources," *IEEE Trans. Wireless Commun.*, vol. 12, no. 12, pp. 6255–6267, Dec. 2013.
- [12] C. Hu, J. Gong, X. Wang, S. Zhou, and Z. Niu, "Optimal green energy utilization in MIMO systems with hybrid energy supplies," *IEEE Trans. Veh. Technol.*, vol. 64, no. 8, pp. 3675–3688, Aug. 2015.
- [13] D. W. K. Ng, E. S. Lo, and R. Schober, "Energy-efficient resource allocation in OFDMA systems with hybrid energy harvesting base station," *IEEE Trans. Wireless Commun.*, vol. 12, no. 7, pp. 3412–3427, Jul. 2013.
- [14] Y. Dong, F. Frnia, and A. Özgür, "Near optimal energy control and approximate capacity of energy harvesting communication," *IEEE J. Sel. Areas Commun.*, vol. 33, no. 3, pp. 540–557, Mar. 2015.
- [15] G. R. Terrell, *Mathematical Statistics: A Unified Introduction*. New York, NY, USA: Springer, 1999.
- [16] G. Yang, C. K. Ho, R. Zhang, and Y. L. Guan, "Throughput optimization for massive MIMO systems powered by wireless energy transfer," *IEEE J. Sel. Areas Commun.*, vol. 33, no. 8, pp. 1640–1650, Aug. 2015.
- [17] L. Liu, R. Zhang, and K.-C. Chua, "Multi-antenna wireless powered communication with energy beamforming," *IEEE Trans. Commun.*, vol. 62, no. 12, pp. 4349–4361, Dec. 2014.

- [18] H. Ju and R. Zhang, "Optimal resource allocation in full-duplex wireless-powered communication network," *IEEE Trans. Commun.*, vol. 62, no. 10, pp. 3528–3540, Oct. 2014.
- [19] K. Huang and V. K. N. Lau, "Enabling wireless power transfer in cellular networks: Architecture, modeling and deployment," *IEEE Trans. Wireless Commun.*, vol. 13, no. 2, pp. 902–912, Feb. 2014.
- [20] I. Flint, X. Lu, N. Privault, D. Niyato, and P. Wang, "Performance analysis of ambient RF energy harvesting: A stochastic geometry approach," in *Proc. IEEE Global Commun. Conf.*, Austin, TX, USA, Dec. 2014, pp. 1448–1453.
- [21] H. Liu, X. Li, R. Vaddi, K. Ma, S. Datta, and V. Narayanan, "Tunnel FET RF rectifier design for energy harvesting applications," *IEEE J. Emerg. Sel. Topics Circuits Syst.*, vol. 4, no. 4, pp. 400–411, Dec. 2014.
- [22] C. Shen, T. H. Chang, K. Y. Wang, Z. Qiu, and C. Y. Chi, "Distributed robust multicell coordinated beamforming with imperfect CSI: An ADMM approach," *IEEE Trans. Signal Process.*, vol. 60, no. 6, pp. 2988–3003, Jun. 2012.
- [23] E. Biglieri, J. Proakis, and S. Shamai, "Fading channels: Information-theoretic and communications aspects," *IEEE Trans. Inf. Theory*, vol. 44, no. 6, pp. 2619–2692, Oct. 1998.
- [24] R. Zhang and C. K. Ho, "MIMO broadcasting for simultaneous wireless information and power transfer," *IEEE Trans. Wireless Commun.*, vol. 12, no. 5, pp. 1989–2001, May 2013.
- [25] M. Kang and M.-S. Alouini, "Largest eigenvalue of complex Wishart matrices and performance analysis of MIMO MRC systems," *IEEE J. Sel. Areas Commun.*, vol. 21, no. 3, pp. 418–426, Apr. 2003.
- [26] A. Maaref and S. Aissa, "Closed-form expressions for the outage and ergodic Shannon capacity of MIMO MRC systems," *IEEE Trans. Commun.*, vol. 53, no. 7, pp. 1092–1095, Jul. 2005.
- [27] E. Boshkovska, D. W. K. Ng, N. Zlatanov, and R. Schober, "Practical non-linear energy harvesting model and resource allocation for SWIPT systems," *IEEE Commun. Lett.*, vol. 19, no. 12, pp. 2082–2085, Dec. 2015.
- [28] J. Guo, H. Zhang, and X. Zhu, "Theoretical analysis of RF-DC conversion efficiency for class-F rectifiers," *IEEE Trans. Microw. Theory Techn.*, vol. 62, no. 4, pp. 977–985, Apr. 2014.
- [29] D. P. Bertsekas, *Dynamic Programming and Optimal Control*, 3rd ed. Belmont, MA, USA: Athena Scientific, 2006.
- [30] Y. Jiang, J. Li, and W. W. Hager, "Joint transceiver design for MIMO communications using geometric mean decomposition," *IEEE Trans. Signal Process.*, vol. 53, no. 10, pp. 3791–3803, Oct. 2005.
- [31] S. Boyd and L. Vandenberghe, *Convex Optimization*. New York, NY, USA: Cambridge Univ., 2004.
- [32] J. Fan, Z. Xu, and G. Y. Li, "Performance analysis of MU-MIMO in downlink cellular networks," *IEEE Commun. Lett.*, vol. 19, no. 2, pp. 223–226, Feb. 2015.
- [33] R. W. Heath, Jr., T. Wu, Y. H. Kwon, and A. C. K. Soong, "Multiuser MIMO in distributed antenna systems with out-of-cell interference," *IEEE Trans. Signal Process.*, vol. 59, no. 10, pp. 4885–4899, Oct. 2011.
- [34] S. Khakurel, C. Leung, and T. Le-Ngoc, "A generalized water-filling algorithm with linear complexity and finite convergence time," *IEEE Wireless Commun. Lett.*, vol. 3, no. 2, pp. 225–228, Apr. 2014.
- [35] S. Sun, Q. Gao, Y. Peng, Y. Wang, and L. Song, "Interference management through CoMP in 3GPP LTE-advanced networks," *IEEE Wireless Commun.*, vol. 20, no. 1, pp. 59–66, Feb. 2013.
- [36] J. Meinilä *et al.*, "WINNER II channel models," in *Radio Technologies and Concepts for IMT-Advanced*. Hoboken, NJ, USA: Wiley, 2009, pp. 39–92.
- [37] K. Nishida *et al.*, "5.8 GHz high sensitivity rectenna array," in *Proc. Int. Microw. Workshop Ser. Innovative Wireless Power Transmiss., Technol., Syst., Appl.*, 2011, pp. 19–22.



**Kai Liang** received the B.S. degree in communication engineering from Xi'an University of Architecture and Technology, Xi'an, China, in 2007, and the Ph.D. degree in communication and information system from Xidian University, Xi'an, China, in 2016.

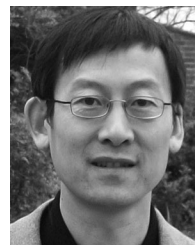
He is a Postdoctoral Fellow with the State Key Laboratory of Integrated Service Networks, Xidian University. From September 2014 to September 2015, he received the funding from the program of China Scholarships Council to visit the Network Convergence Laboratory, University of Essex, Colchester, U.K. His research interests include broadband wireless access, wireless network design, coordinated multipoint-to-multiuser communication systems, and fog computing.



**Liqiang Zhao** (M'12) received the B.Eng. degree in electrical engineering from Shanghai Jiao Tong University, Shanghai, China, in 1992, and the M.Sc. degree in communications and information systems and Ph.D. degree in information and communications engineering from Xidian University, Xi'an, China, in 2000 and 2003, respectively.

From 1992 to 2005, he was a Senior Research Engineer with the 20th Research Institute, Chinese Electronics Technology Group Corporation, China, where his research focused on mobile communication systems and spread spectrum communications. From 2005 to 2007, he was an Associate Professor with the State Key Laboratory of Integrated Service Networks, Xidian University, where his research focused on WiMAX, WLAN, and wireless sensor networks. In June 2007, he was appointed as a Marie Curie Research Fellow with the Centre for Wireless Network Design, University of Bedfordshire, to conduct research in the GAWIND project funded under the EU FP6 HRM program. His activities focused on the area of automatic wireless broadband access network planning and optimization. Since June 2008, he has been with Xidian University, where he has been a Professor of information and communication engineering. His current research focuses on 5G, aerospace communications, and nanonetworks.

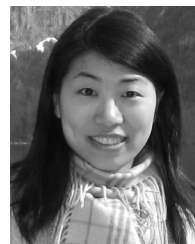
Dr. Zhao has been awarded more than 20 projects funded by a number of sources, government, and direct industrial funding since 2005. His participation in various projects has yielded a number of concrete results including enormous high-level publications, etc. Due to his excellent works in education and research, he was awarded by the Program for New Century Excellent Talents in University, Ministry of Education, China, in 2008.



**Kun Yang** (SM'08) received the B.Sc. degree in computer science and M.Sc. degree in computer networks from Jilin University, Changchun, China, in 1991 and 1994, respectively, and the Ph.D. degree in networks and service management from University College London (UCL), London, U.K., in 2006.

He is currently a Chair Professor with the School of Computer Science and Electronic Engineering, University of Essex, Colchester, U.K., leading the Network Convergence Laboratory. He is also an Affiliated Professor with the University of Electronic Science and Technology of China, Chengdu, China. Before joining the University of Essex at 2003, he worked at UCL on several European Union (EU) research projects for several years. He manages research projects funded by various sources such as UK EPSRC, EU FP7/H2020, and industries. He has published more than 100 journal papers. His research interests include wireless networks, future Internet technology and network virtualization, and mobile cloud computing and networking.

Dr. Yang is a Fellow of IET. He serves on the editorial boards of both IEEE and non-IEEE journals.



**Xiaoli Chu** (M'06–SM'15) received the B.Eng. degree in electronic and information engineering from Xi'an Jiao Tong University, Xi'an, China, in 2001, and the Ph.D. degree in electrical and electronic engineering from the Hong Kong University of Science and Technology, Hong Kong, in 2005.

She is a Senior Lecturer with the Department of Electronic and Electrical Engineering, University of Sheffield, Sheffield, U.K. From September 2005 to April 2012, she was with the Centre for Telecommunications Research, Kings College London. She has published more than 100 peer-reviewed journal and conference papers. She is the Lead Editor/author of the book *Heterogeneous Cellular Networks: Theory, Simulation and Deployment* (Cambridge University Press, 2013) and the book *4G Femtocells: Resource Allocation and Interference Management* (Springer 2013).

Dr. Chu is an Editor of IEEE WIRELESS COMMUNICATIONS LETTERS and an Editorial Board Member of the IEEE ComSoc MMTTC R-Letter. She was a Guest Editor of the IEEE TRANSACTIONS ON VEHICULAR TECHNOLOGY and the *ACM/Springer Journal of Mobile Networks & Applications*. She was a Co-Chair of the Wireless Communications Symposium for the IEEE International Conference on Communications 2015, Workshop Co-Chair for the IEEE International Conference on Green Computing and Communications 2013, and has been the Technical Program Committee Co-Chair of several workshops on heterogeneous networks for IEEE ICC, GLOBECOM, WCNC, PIMRC, etc.